Since January 2020 Elsevier has created a COVID-19 resource centre with free information in English and Mandarin on the novel coronavirus COVID-19. The COVID-19 resource centre is hosted on Elsevier Connect, the company's public news and information website.

Respiratory Physiology & Neurobiology 309 (2023) 104000

Contents lists available at ScienceDirect

Respiratory Physiology & Neurobiology

journal homepage: www.elsevier.com/locate/resphysiol

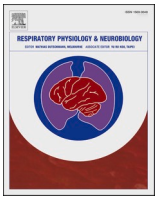

Morphological and functional findings in COVID-19 lung disease as compared to Pneumonia, ARDS, and High-Altitude Pulmonary Edema

Gustavo R. Zubieta-Calleja [a], Natalia Zubieta-DeUrioste [a], Felipe de Jesús Montelongo [b], Manuel Gabriel Romo Sanchez [b], Aurio Fajardo Campoverdi [c], Patricia Rieken Macedo Rocco [d,e], Denise Battaglini [f,*], Lorenzo Ball [f,g], Paolo Pelosi [f,g]

[a] High Altitude Pulmonary and Pathology Institute (HAPPI - IPPA), La Paz, Bolivia
[b] Critical and Neurointensive Care Unit and Pathology Department, Hospital General de Ecatepec "Las Américas", Instituto de Salud del Estado de México, México
[c] Critical Care Unit, Viña del Mar, Chile
[d] Laboratory of Pulmonary Investigation, Carlos Chagas Filho Institute of Biophysics, Federal University of Rio de Janeiro, Rio de Janeiro, Brazil
[e] COVID-19 Virus Network, Ministry of Science, Technology, and Innovation, Brasilia, Brazil
[f] Anesthesia and Intensive Care, San Martino Policlinico Hospital, IRCCS for Oncology and Neurosciences, Genoa, Italy
[g] Department of Surgical Sciences and Integrated Diagnostics, University of Genoa, Genoa, Italy

ARTICLE INFO

Keywords:
HAPE
SARS-CoV-2
COVID-19
Lung sequelae
Viral pneumonia
ARDS

ABSTRACT

Coronavirus disease-2019 (COVID-19) may severely affect respiratory function and evolve to life-threatening hypoxia. The clinical experience led to the implementation of standardized protocols assuming similarity to severe acute respiratory syndrome (SARS-CoV-2). Understanding the histopathological and functional patterns is essential to better understand the pathophysiology of COVID-19 and then develop new therapeutic strategies. Epithelial and endothelial cell damage can result from the virus attack, thus leading to immune-mediated response. Pulmonary histopathological findings show the presence of Mallory bodies, alveolar coating cells with nuclear atypia, reactive pneumocytes, reparative fibrosis, intra-alveolar hemorrhage, moderate inflammatory infiltrates, micro-abscesses, microthrombus, hyaline membrane fragments, and emphysema-like lung areas. COVID-19 patients may present different respiratory stages from *silent to critical hypoxemia*, are associated with the degree of pulmonary parenchymal involvement, thus yielding alteration of ventilation and perfusion relationships. This review aims to: discuss the morphological (histopathological and radiological) and functional findings of COVID-19 compared to acute interstitial pneumonia, acute respiratory distress syndrome (ARDS), and high-altitude pulmonary edema (HAPE), four entities that share common clinical traits, but have peculiar pathophysiological features with potential implications to their clinical management.

1. Introduction

Coronavirus disease 2019 (COVID-19) is caused by the severe acute respiratory syndrome coronavirus 2 (SARS-CoV-2) virus (Mitra et al., 2020) and is characterized by flue-type (variable) symptoms that could evolve to severe hypoxemia and subsequent death (Lin et al., 2020). Over 5% of infected patients develop pneumonia followed by acute respiratory distress syndrome (ARDS) thus requiring mechanical ventilation (Ferreira et al., 2021). Mortality has been reported as 0.3 deaths per 1000 cases in patients aged between 5 and 17 years, 305 death per 1000 cases in patients aged 85 or older (Wiersinga et al., 2020). A high incidence of different clinical presentations (Lavinio et al., 2021; Robba et al., 2021b), as well as cardiac (De Marzo et al., 2021), neurologic (Battaglini et al., 2020b), hepatic and renal injury (Lopes-Pacheco et al.,

Abbreviations: AIP, acute interstitial pneumonia; ARDS, acute respiratory distress syndrome; CO_2, carbon dioxide; COVID-19, coronavirus disease 2019; CT, computed tomography; DAD, diffuse alveolar damage; DO_2, oxygen delivery; $ECCO_2R$, extracorporeal carbon dioxide removal; ECMO, extracorporeal membrane oxygenation; FiO_2, fraction of inspired oxygen; HAPE, high altitude pulmonary edema; Hb, hemoglobin; HIF, hypoxia inducible factor; IIP, idiopathic interstitial pneumonia; LUS, lung ultrasound; MODS, multiple organ dysfunction; $PaCO_2$, arterial partial pressure of carbon dioxide; PAO_2, alveolar partial pressure of oxygen; PaO_2, arterial partial pressure of oxygen; PEEP, positive end-expiratory pressure; SARS-CoV-2, severe acute respiratory syndrome coronavirus-2; SpO_2, peripheral saturation of oxygen; V/Q, ventilation/ perfusion; VILI, ventilator-induced lung injury.

* Corresponding author.
E-mail address: battaglini.denise@gmail.com (D. Battaglini).

https://doi.org/10.1016/j.resp.2022.104000
Received 2 October 2022; Received in revised form 18 November 2022; Accepted 27 November 2022
Available online 29 November 2022

2021), have been reported yielding the definition of Multiple Organ Dysfunction Syndrome (MODS)-CoV-2 (Robba et al., 2020b). COVID-19 pneumonia histopathological findings have been reported different from (Batah and Fabro, 2021) or overlapped (Xu et al., 2020) with Acute Interstitial Pneumonia (AIP), ARDS, or High Altitude Pulmonary Edema (HAPE) (Pomara et al., 2020; Zubieta-Calleja and Zubieta-DeUrioste, 2021a, 2021b). These four diseases share similar clinical presentations, but also histopathological characteristics, and radiographic images. However, each of them has peculiar characteristics. Morphological and functional characteristics of these pathologies can vary depending on the specific environment (Zubieta-Calleja et al., 2021; Zubieta-Calleja and Zubieta-DeUrioste, 2022). This review aims to discuss the morphological (histopathological and radiological) and functional findings of COVID-19 compared with pneumonia, ARDS and HAPE as well as possible implications relevant to therapeutic strategies.

2. Histopathological findings

2.1. Acute interstitial pneumonia

Different microorganisms can cause pneumonia *(or pneumonitis),* classically defined as an acute disease marked by inflammation of lung tissue accompanied by infiltration of alveoli and often bronchioles with white blood cells (such as neutrophils) and fibrinous exudate (Travis et al., 2013) (Table 1). The most recent anatomopathological classification dates back to 2013, including the broad definition of idiopathic interstitial pneumonia (IIP), incorporating more than 200 acute or chronic lung diseases with various degrees of inflammation and fibrosis (Travis et al., 2013). AIP is characterized by a severe idiopathic interstitial disease that includes the presence of clinical symptoms, bilateral lung infiltrates on radiographs, and the absence of identifiable etiology (Thille et al., 2013; Travis et al., 2013). In AIP, type I and I epithelial cells may present necrosis, erosion, fibrin exudation and ubiquitin-positive intracytoplasmic inclusion bodies (Mallory bodies) that are ubiquitin positive. AIP may evolve to ARDS and fibrosis (Thille et al., 2013).

Table 1
Comparison of anatomopathological findings in AIP, ARDS, HAPE, and COVID-19.

Disease	Anatomopathological findings
AIP	Lung tissue derangement with alveolar collapse. Hyaline membrane formation. Polymorphonuclear and monocytes infiltration. Pneumocytes characteristics in AIP include epithelial necrosis, erosion, fibrin exudation, Mallory bodies. Pneumocytes Ub+ . Early fibroblastic interstitial fibrosis, septal and para-septal reparative fibrosis.
ARDS	Lung tissue derangement with alveolar collapse. Intra-alveolar and interstitial edema. Necrotic alveolar epithelial cells and exudates of serum proteins from the damaged and leaky capillaries. Alveolar type I cell necrosis, alveolar type II cell proliferation, interstitial proliferation of fibroblast and myofibroblast or organizing interstitial fibrosis. Hyaline tissue formation. Reactive pneumocytes with nuclear atypia and hyperplasia. Mallory like inclusions in type 2 pneumocytes (Ub+). Scattered neutrophilic infiltrates localized to terminal bronchioles and surrounding alveoli with evident confluence of infiltrates between adjacent lobules. Thrombi are common in small/ medium pulmonary arterioles. Abundant fibroblast in the interstitium, fibrosis and interstitial thickening by fibroblasts.
HAPE	Diffuse alveolar edema including red blood cells, polymorphonuclear cells, and macrophages. Widened septa due to interstitial edema. Occasional alveolar hyaline membranes. Type II pneumocytes could be damaged (due to stress failure) and pulmonary surfactant impaired. Congested pulmonary arterioles and capillaries. Intra-alveolar hemorrhage is present in scattered areas of lung parenchyma, particularly in the more severe cases. Thrombi and fibrin clots plugging arterioles and capillaries.
COVID-19	Lung tissue derangement with alveolar collapse. Intra-alveolar hemorrhage. Alveolar rupture. Hyaline tissue formation. Polymorphonuclear and monocytes infiltration. Active viral replication within type 2 pneumocytes Reactive pneumocytes with nuclear atypia and hyperplasia. Mallory like intracytoplasmic inclusions in type 2 pneumocytes. Masson's bodies. Microthrombi, vasculitis or vascular thrombosis. Early fibroblastic interstitial fibrosis, septal and para-septal reparative fibrosis.

Table Legend: AIP, acute interstitial pneumonia; ARDS, Acute Respiratory Distress Syndrome; COVID-19, Coronavirus disease 2019; HAPE, high-altitude pulmonary edema.

2.2. ARDS

Diffuse alveolar damage (DAD) is considered the histological hallmark for the acute phase of ARDS (Table 1). DAD can present as typical histologic evolution of AIP, but the clinical evolution of AIP and DAD are different. Indeed, AIP and DAD constitute two independent entities that often coexist (Cardinal-Fernández et al., 2017). Three phases of traditional ARDS have been identified: 1) acute phase (<48 h) with interstitial and alveolar edema, 2) subacute phase (days 3–7) with the formation of hyaline membranes and fibrin deposits, and 3) proliferative phase (>7 days) with abundant fibroblast in the interstitium, fibrosis, and hyperplasia of type II pneumocytes (Mukhopadhyay and Parambil, 2012). Hyaline membrane formation and DAD with fibrin exudation and intraluminal granulation can be maintained due to epithelial cell damage (Guerin et al., 2015). Lung histopathology differs in "pulmonary and "extrapulmonary" ARDS (Pelosi et al., 2003), although both are characterized by increased lung weight compared to normal lungs (1.700–2.500 gr vs 800 gr, respectively) and presence of DAD, albeit with different distribution. Pulmonary ARDS primarily affects the alveolar epithelium, with damage occurring mainly in the intra-alveolar space, with alveolar flooding and areas of consolidation (Menezes et al., 2005; Rocco and Pelosi, 2008). In extrapulmonary ARDS, vascular endothelial cells are the first target of damage, with a subsequent increase in vascular permeability. The main pathologic alteration due to an indirect insult may be micro-vessel congestion and interstitial edema, with relative sparing of intra-alveolar spaces. The histopathological distinction between "pulmonary" and "extrapulmonary" ARDS has not been always feasible due to the frequent overlapping of these two clinical situations (Gattinoni et al., 2001; Goodman et al., 1999). DAD might evolve to fibrosis regardless of the underlying lung condition; however, its frequency, specific findings and pathogenesis might be disease-specific (Ackermann et al., 2020; Ball et al., 2021a; Kamp et al., 2022).

2.3. High altitude pulmonary edema

HAPE is a non-cardiogenic pulmonary edema that develops after exposure to high altitudes (> 1700 – 2000 m above sea level) (Giesenhagen et al., 2019). It is assumed that there exists a genetic predisposition to HAPE and this might be associated with an exaggerated vascular response in patients susceptible to hypoxia and poor outcome in those with COVID-19 (Garrido et al., 2022). Histological findings of HAPE include marked diffused alveolar edema, congested pulmonary arterioles and capillaries, and occasional alveolar hyaline membranes (Droma et al., 2001) (Table 1). In most severe cases, histological findings may be compatible with DAD. In particular, the alveolar spaces are often distended with edema extended to alveoli, alveolar ducts, sacs, and respiratory bronchioles. The edema includes red blood cells, polymorphonuclear cells, and macrophages. Additionally, alveolar capillaries and pulmonary arterioles are congested with stasis. Intra-alveolar hemorrhage can be present in scattered areas of lung parenchyma in the more severe cases. Thrombi and fibrin clots plugging arterioles and

capillaries can occasionally be found. The alveolar structures are usually maintained, but the septa are widened due to interstitial edema, while hyaline membranes can be eventually observed (Droma et al., 2001). HAPE is clearly associated with pulmonary artery hypertension, which manifests with changes in the pulmonary vascular endothelium characterized by 1) a transition form, from a quiescent state to an activated state with acquisition of adhesive capacity, 2) an aberrant proliferative and apoptosis-resistant phenotype, 3) a pro-inflammatory phenotype with the release of cytokines and chemokines, and 4) a fibrotic phenotype with the release of growth factors, angiotensin, and leptin (Huertas et al., 2018). Type II epithelial cells could be damaged and pulmonary surfactant impaired (Droma et al., 2001). Nevertheless, these lung histological changes reverse within 24 h in younger patients and up to several days in older patients, never resulting in fibrosis.

2.4. COVID-19 pneumonia

Lung histopathology in COVID-19 pneumonia (Edler et al., 2020; Hanley et al., 2020; Pomara et al., 2020) is characterized by an inflammatory process (neutrophil and mononuclear cell infiltration), alveolar destruction and collapse, hyaline tissue formation, microhemorrhages, and micro-abscess possibly due to superinfection, which can result in extensive disruption of the lung parenchyma (Zubieta--Calleja and Zubieta-DeUrioste, 2021b). Pathological findings in the cells include intra-alveolar Masson Bodies, which are a typical hallmark of organizing pneumonia. Nuclear atypia of epithelial cells is also present (Zubieta-Calleja and Zubieta-DeUrioste, 2021b) (Table 1). Severe COVID-19 pneumonia shares some pathological similarities with “pulmonary” ARDS characterized by lung inflammation, presence of consolidation, some areas of atelectasis, changes in vascular permeability, and hypoxemia (Ackermann et al., 2020; Ranieri et al., 2012). Autopsy findings in severe COVID-19 pneumonia patients reveals the presence of DAD, fibrosis, bullae-filled necrotic lung tissue, chronic lung inflammation, edema in the bronchial mucosa, and thromboembolic events (Barisione et al., 2021; Barton et al., 2020; Edler et al., 2020; Wichmann et al., 2020). Three phases, similar to the traditional DAD, have been identified: 1) the acute/early exudative phase that is characterized by intra-alveolar edema and interstitial widening, with a peak of hyaline membrane (both diffuse and focal) formation 4–5 days after initial insult (Angeles Montero-Fernandez and Pardo-Garcia, 2021); 2) an organizing/mid proliferative phase, which is characterized by cellular fibroblastic proliferation, type II epithelial cell hyperplasia, and squamous metaplasia; and 3) late/fibrous phase DAD with honeycombing (Barisione et al., 2020). The hyaline membranes are in this stage fused into the alveolar septa and not easily recognizable (Angeles Montero-Fernandez and Pardo-Garcia, 2021). Post-mortem transbronchial lung cryobiopsies during mechanical ventilation confirmed the presence of "pneumocyte loss” (pneumolysis) with discontinuation of the alveolar epithelial lining, hyaline membranes, intra-alveolar fibrinous exudate, early interstitial fibrosis, obliteration of the alveolar structure by fibrosis, type 2 epithelial cell hyperplasia and atypia, Mallory-like intracytoplasmic inclusions in type 2 epithelial cells, micro-honeycombing, foci of bronchopneumonia, associated with vascularlysis, vasculitis or vascular thrombosis (Barisione et al., 2020). Vascular microthrombosis was described in conventional ARDS but occurs more frequently in COVID-19 (Ackermann et al., 2020).

2.4.1. Parenchymal destruction in severe COVID-19 pneumonia

Parenchymal destruction is the most severe evolution of COVID-19 pneumonia (Zubieta-Calleja and Zubieta-DeUrioste, 2021b). Irreversible remodeling of lung parenchyma, with fibrotic tissue adhering to the parietal pleura, was firstly described in pulmonary tuberculosis (Hall, 1938). It was therefore observed in COVID-19, in the context of a disease evolving to progressive hypoxemia, subsequent hypercapnia, and altered shunt (Zubieta-Calleja et al., 2021). A gel-like fluid has been found in autopsy lung samples in COVID-19, and the presence of hyaluronan has been reported (Hellman et al., 2020). COVID-19 patients present initially a predominance of advanced lesions in the lower lobes of both lungs. The probable explanation could be associated with aerodynamics and lung elasticity that initially respond with lower lobes distention on inhalation due to diaphragmatic contraction and direct main bronchi orientation, driving the SARS-CoV-2 directly to impact the lungs in that area (Yan et al., 2020). These findings in COVID-19 differentiates itself from HAPE, which occurs on a rapid ascent to high altitude in some individuals who can present an arterial partial pressure of oxygen (PaO_2) as low as 30 mmHg but can fully recover within a few days. Also, in COVID-19, there is lung pneumocyte destruction followed by inflammation. HAPE-like edema, and some minor hemorrhage, giving rise to severe lung damage. However, HAPE-like edema in COVID-19 could be concomitantly present since the exclusion and destruction of respiratory units reduces the gas exchange surface significantly, simulating a high-altitude abrupt ascent. The normal remaining lung tissue can suffer edema as it results from extreme hypoxia, pulmonary hypertension, and stress failure of capillaries. The brownish color of the lungs probably results from the iron deposit due to hemolysis in the interstitium where fibrosis is forming.

3. Radiological findings

3.1. Acute interstitial pneumonia

Chest radiograph in AIP shows bilateral opacifications with air bronchograms and sparing of the costophrenic angles. Consolidation can appear during the organizing phase with a possible ground glass appearance and irregular lung opacities (Primack et al., 1993). Chest computed tomography (CT) findings of AIP patients reveal ground glass attenuation areas with a mosaic pattern and air space consolidation in dependent areas. This pattern results from alveolar septal edema, and hyaline membrane formation at histology, which are typical of the exudative phase (Palmucci et al., 2014). These signs are commonly bibasilar, sometimes diffuse or localized to the upper lobes. Intra-alveolar fibrosis with consolidation can be identified in the organizing phase with possible bronchiectasis formation and cyst. The latter are more common in the non-dependent lung areas (Palmucci et al., 2014) (Table 2).

3.2. ARDS

Studies have described morphological differences at chest CT scan in patients with pulmonary and extrapulmonary ARDS (Gattinoni et al., 2001; Goodman et al., 1999). “Pulmonary” ARDS appears to be asymmetric, with a mix of consolidation and ground-glass opacification, while “extrapulmonary” ARDS presents a symmetric ground-glass opacification. However, to date there has been no tomographic characteristic able to predict the etiology of ARDS (Desai et al., 1999), since direct and indirect injuries can coexist, making interpretation of the morphological pattern more difficult. In the organizing and fibrotic phase, traction bronchiectasis and reticulation may develop with an anterior predominance (Obadina et al., 2013) (Table 2). Typical patterns at CT scan in “pulmonary” and “secondary” ARDS are shown in Fig. 1.

3.3. High altitude pulmonary edema

Chest radiograph of patients with HAPE presents distinct patterns which can often be confused with cardiopulmonary diseases (Nair et al., 2021). Unilateral or bilateral asymmetrical alveolar-interstitial opacities with relative sparing of the periphery and apices have been identified in some patients (Zubieta-Calleja and Zubieta-DeUrioste, 2021a). The opacities could be marginated, and the distribution patchy, with initial confluence in the perihilar region, and prominent horizontal fissure. Other images showed lobar consolidation, limited by a horizontal fissure. Focal patchy air-space opacities/ consolidations, thus mimicking

Table 2
Comparison of radiological findings in AIP, ARDS, HAPE, and COVID-19.

Disease	Radiological findings
AIP	Ground grass attenuation areas with a mosaic pattern and air space consolidation in dependent areas, bibasilar, diffuse or localized in the upper lobes. Intra-alveolar fibrosis with consolidation in the organizing phase with possible bronchiectasis formation and cyst, especially in the non-dependent lung areas.
	In "pulmonary" ARDS appearance is asymmetric, with a mix of consolidation and ground-glass opacification, possible pleural effusion, and emphysema. Predominance of air bronchograms and pneumomediastinum
	In "extrapulmonary" ARDS predominantly symmetric ground-glass opacification are present with possible pleural effusion and emphysema. Ground-glass opalization and consolidation are greater in the central third of the lung than in the sternal or vertebral third without significant craniocaudal predominance. Consolidation is mainly distributed in the middle and basal levels as well as the vertebral position.
ARDS	Heterogenous foci of consolidation, ground-glass opacities (with gravitational gradient), and crazy paving, with predominance in the posterior and basal areas. Possible air bronchograms and small pleural effusions.
	In the organizing and fibrotic phase, traction bronchiectasis and reticulation may develop (anterior predominance).
HAPE	Unilateral or Bilateral asymmetrical alveolo-interstitial opacities with relative sparing of the periphery and apices, usually marginated, with patchy distribution and initial confluence in the perihilar region, and prominent horizontal fissure, interlaced with normally aerated areas. Possible lobar consolidation limited by horizontal fissure. Focal patchy air-space opacities/ consolidations. Pulmonary edema usually occurs in areas of high blood flow, with a patchy distribution.
COVID-19	Phenotype 1 (or L) usually presents as multiple focal over perfused ground glass opacities and normally aerated areas and is prevalent of mild to moderate diseases. Possible diversion of ventilation toward non-dependent aerated lung regions and reduction in pulmonary perfusion due to increased airway pressure, collapse of capillaries and/or microthrombosis and formation of no recruitable atelectasis.
	Phenotype 2 (or H) shows a patchy ARDS-like pattern, with inhomogeneously distributed and hyper/hypo-perfused areas that is prevalent of severe disease. Increased lung weight and consolidated and non-aerated lung regions mainly distributed in the dependent lung regions. In these clinical conditions, areas with low V/Q persist but associated with areas of "true shunt".
	Phenotype (F) which represents a final evolution to fibrosis.

Table Legend: AIP, acute interstitial pneumonia; ARDS, Acute Respiratory Distress Syndrome; COVID-19, Coronavirus disease 2019. HAPE, high-altitude pulmonary edema.

a tuberculosis-type pattern. Additionally, bilateral symmetrical perihilar or diffuse opacities were noted in some cases, although a monolateral diffuse opacity can be also identified (Nair et al., 2021). Perfusion scans and magnetic resonances of patients with HAPE show that pulmonary edema occurs in areas of high blood flow, with a patchy distribution (Dehnert et al., 2006; Hopkins et al., 2005). Typical patterns of HAPE identified at CT scan are shown in Fig. 2 and Table 2.

3.4. COVID-19 pneumonia

Distinct COVID-19 pneumonia phenotypes have been identified in the chest CT, including 1) a phenotype 1 (or L) (Gattinoni et al., 2020; Robba et al., 2020a) that presents as multiple focal over perfused ground glass opacities receiving more perfusion than ventilation and normally aerated areas, and is prevalent of mild to moderate diseases. In this case, possible diversion of ventilation toward non-dependent aerated lung regions and reduction in pulmonary perfusion due to increased airway pressure, the collapse of capillaries and/or micro-thrombosis and formation of non-recruitable consolidation can appear; 2) a phenotype 2 (or H) (Gattinoni et al., 2020; Robba et al., 2020a) that shows a patchy ARDS-like pattern, with inhomogeneously distributed and hyper/hypo-perfused areas that are associated with severe disease (Gattinoni et al., 2020; Orlandi et al., 2021). In this case, the lung weight can be increased with consolidated and non-aerated lung regions mainly distributed in the dependent lung regions. Areas with low ventilation/perfusion (V/Q) persist, but are associated with "true shunt" areas; 3) A phenotype (F) which represents a final evolution to fibrosis (Gattinoni et al., 2020; Robba et al., 2020a; Tonelli et al., 2021). The incidence rate of each COVID-19 phenotype was 62% and 10% for 1 and 2 phenotypes, respectively, in severe COVID-19 patients. Chest CT and lung ultrasound imaging (LUS) differed between survivors (mostly phenotype 1) and non-survivors (mostly phenotype 2) and were associated with ICU mortality (Orlandi et al., 2021). Moreover, chest CT positively correlates with lung ultrasound findings suggesting that it can be a valuable monitoring tool in critically ill settings for daily monitoring (Orlandi et al., 2021) (Table 2). Fig. 3 presents typical patterns of COVID-19 phenotype 1 and phenotype 2 at CT scan.

4. Gas-exchange: general principles

AIP, ARDS, HAPE, and COVID-19 pneumonia present similar symptoms. However, a careful evaluation could identify some minimal or marked differences in the diagnostic criteria, definition, gas-exchange abnormalities, and clinical manifestations. In normal lung, gas-exchange is determined by the greater amount of normally aerated and perfused alveoli, with low venous admixture and wasted ventilation. Matching between ventilation (V') and perfusion (Q') of lung regions is the main determinant of gas-exchange (Petersson and Glenny, 2014). Venous admixture, mainly impairing oxygenation, is determined by lung areas with lower V'/Q' ratios and/or true shunt (Petersson and Glenny, 2014). In normal lungs, a continuous distribution of alveoli from lower (0.001) to higher (10) V/Q areas are present following a gaussian shape, while it may present skewness in pathological conditions. In normal lungs, lung areas with extremely low V'/Q'are less frequent, while those with V'/Q' between 1 and 0.1 are predominant. On the other hand, lung areas of "true shunt" are minimal and mostly due to anatomical shunt (3–5%). This means that in normal conditions, breathing in air, the oxygen content and arterial partial pressure of

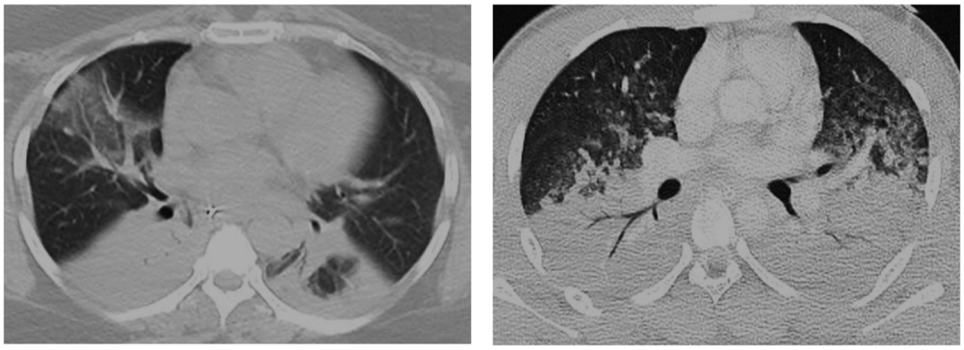

Fig. 1. Typical pattern of "pulmonary" (left) and "secondary" (right) ARDS at CT scan.

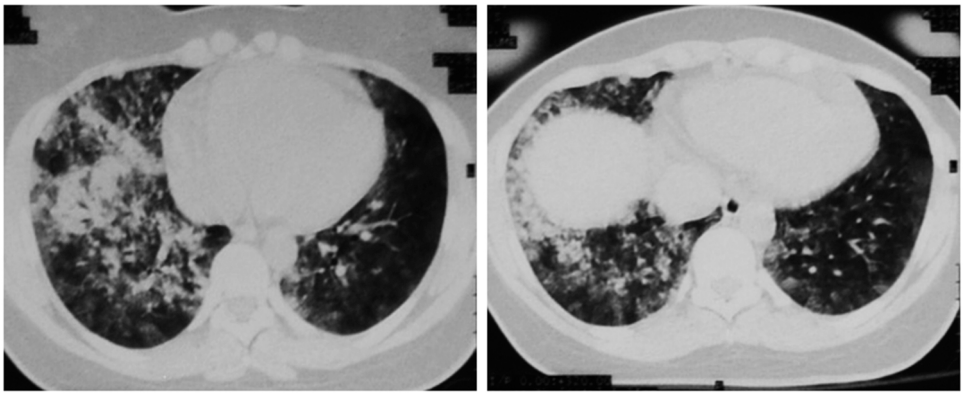

Fig. 2. Typical patterns of HAPE identified at CT scan of a young woman after her arrival in La Paz, Bolivia at 3500 m. Note the patchy and bilateral presentation of edema, areas where oxygen transport to pulmonary capillaries is severely compromised, generating low V'/Q' areas responsible for the severe hypoxemia that can be encountered. The patient evolved favorably in 3 days and was able to fly back home on a scheduled flight, without sequalae.

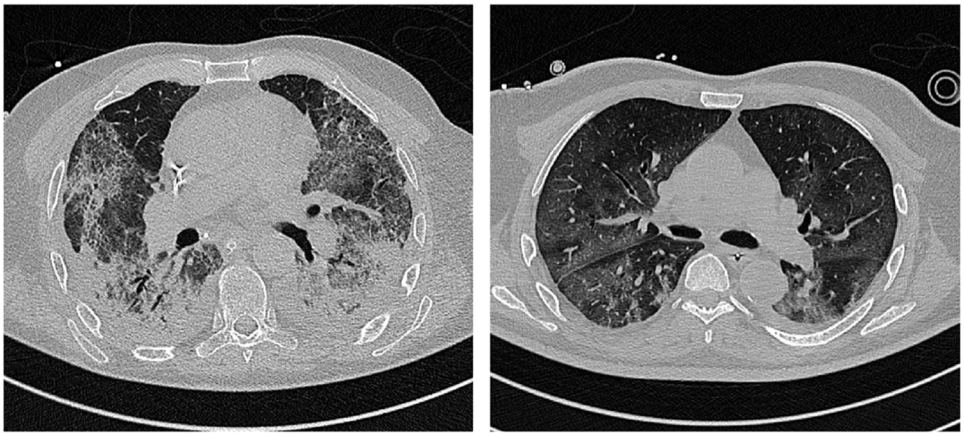

Fig. 3. Typical pattern of COVID-19 phenotype 1 and 2. This figure depicts typical patterns of COVID-19 with preserved elastance (phenotype 1, left) and increased elastance (phenotype 2, right) at CT scan.

oxygen (PaO_2) are only slightly lower than alveolar PO_2 (PAO_2) leading to low PAO_2-PaO_2 difference (Petersson and Glenny, 2014). In pathological conditions, when lung areas present extremely low V'/Q' ratios, the oxygen content, as well as PaO_2 decrease, while the PAO_2-PaO_2 difference increases (Fajardo et al., 2020). Thus, administering higher inspiratory oxygen fractions, in the presence of increased venous

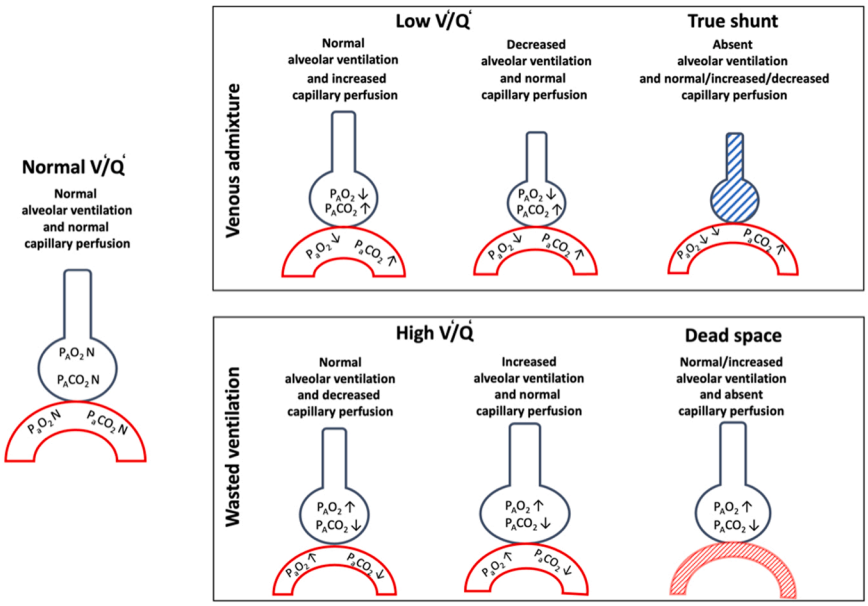

Fig. 4. Changes in gas exchange according to ventilation/perfusion. This figure depicts changes in gas exchange according to ventilation (V')/perfusion (Q') alterations. On the left, normal gas exchange with normal V'/Q'. Above, venous admixture with three possible conditions: 1) low V'/Q' with normal alveolar ventilation and increased capillary perfusion; 2) low V'/Q' with decreased alveolar ventilation and normal capillary perfusion; and 3) true shunt with absent alveolar ventilation and variable capillary perfusion. Below, wasted ventilation with three possible conditions: 1) high V'/Q' with normal alveolar ventilation and decreased capillary perfusion; 2) high V'/Q' with normal capillary perfusion, and 3) dead space with normal capillary ventilation but absent perfusion.

admixture mainly due to lower V'/Q', the oxygen content and PaO_2 increase while the PAO_2-PaO_2 difference decreases. This is explained by the fact that alveoli with low V'/Q' areas are open to inspiratory gases and may be reached by increased FiO_2 (Petersson and Glenny, 2014). On the other hand, in pathological conditions, when extremely high "true shunt" predominated, while breathing ambient air, the oxygen content as well as PaO_2 decrease while the PAO_2-PaO_2 increases similarly or even greater compared to low V'/Q'. However, administering higher inspiratory oxygen fractions in the presence of increased venous admixture mainly due to higher "true shunt", the oxygen content, as well as PaO_2, minimally increase while the PAO_2-PaO_2 gradient minimally decreases (Karbing et al., 2020) (Fig. 4). This is explained by the fact that in the presence of increased venous admixture mainly is due to increased "true" shunt, although some alveoli may contain a high fraction of inspired oxygen (FiO_2), but the oxygen within them cannot diffuse into the capillaries that are closed (shunt) (Fig. 4). Wasted ventilation is due to high V'/Q' areas as well as increased dead space (areas ventilated but not perfused), resulting predominantly in impairment of CO_2 removal. In these lung regions, alveolar oxygenation depends on inspired oxygen fraction, but the effectiveness of carbon dioxide (CO_2) washout is impaired by lower (high V'/Q') or absent (dead space) perfusion. These areas represent part of the lung that do not contribute to increased oxygen content or PaO_2 while impairing CO_2 washout yield increased inspiratory wasted effort (Karbing et al., 2020). A high $PaCO_2$ reduces the hypoxia tolerance, further aggravating the deleterious effects of hypoxia (Zubieta-Calleja et al., 2013). Fig. 5 depicts the response of V'/Q' to increased FiO_2, while Fig. 6 depicts possible V'/Q' distribution in different pathological conditions.

4.1. Acute interstitial pneumonia

In AIP, hypoxemia is mainly associated with increased lung weight, lung consolidation, and increased intrapulmonary shunt. Consolidation may be localized or widely distributed along the ventral-dorsal gradient or in the dependent lung regions in the supine position. On the other hand, the perfusion is mainly gravity-dependent (similar to ARDS), yielding increased venous admixture due to true shunt (Dakin et al., 2011). The lung areas of low V'/Q' are present but not markedly affecting gas-exchange impairment. On the other hand, increased wasted ventilation due to the combination of high alveolar dead space and high V'/Q' may be present mainly due to diversion of ventilation toward non-dependent aerated lung regions and reduction in pulmonary perfusion due to increased airway pressure or micro-thrombosis. V'/Q' ratio in patients with interstitial pneumonia was firstly described many years ago. V'/Q' profile in sub-pleural lung zones with high V'/Q' ratios and dead space (wasted ventilation) showed flattened peaks with broadened V'/Q' distribution (Suga et al., 2009) (Fig. 6).

4.2. ARDS

In ARDS, higher regional perfusion and true shunt are in the dependent lung regions [11] and edema follows a ventral-dorsal gradient [12] with prevalent low V'/Q' and shunt (Fig. 6). The pressure applied on dependent lung regions favors progressive atelectasis formation (Pelosi et al., 1994), while positive end-expiratory pressure (PEEP) keeps the dependent alveoli open, improving gas-exchange and respiratory system compliance (Gattinoni et al., 1994). Hypoxemia is mainly associated with increased lung weight and atelectasis, yielding increased intrapulmonary shunt. Atelectasis is localized in the dependent lung regions in the supine position. In this clinical condition, the perfusion is mainly gravity-dependent, and the venous admixture is primarily due to true shunt (Dakin et al., 2011). In pulmonary ARDS, there are some lung regions with lower V'/Q', which do not markedly affect gas-exchange. Moreover, there are areas of increased dead space.

4.3. High altitude pulmonary edema

The pathophysiology of HAPE involves a reduced environmental partial pressure of inspired oxygen causing hypoxic pulmonary vasoconstriction that leads to an increased pulmonary arterial pressure with focalized higher pulmonary vascular resistances, higher heart rate and lower arterial oxygen saturation (Chanana et al., 2020). The etiopathology of HAPE is not clear and several hypothesis have been described: 1) genetic predisposition; 2) changes in renin-angiotensin-aldosterone system (RAS), since aldosterone increases the retention of extracellular fluid (Chanana et al., 2020); 3) modifications in nitric oxide (NO), which usually maintains the pulmonary vascular homeostasis; 4) different expression of hypoxia-inducible factor (HIF)− 1 that exponentially increases when the cellular oxygen is low (Chanana et al., 2020); 5) viral infection which may explain the similar pattern observed in COVID-19 pneumonia (Zubieta-Calleja, 1989). The tongue in HAPE has very similar characteristics to the tongue in COVID-19. Clinical symptoms of HAPE include dyspnea, frothy pink sputum, tachypnea, persistent cough, cyanosis, and tachycardia (Chanana et al., 2020). The

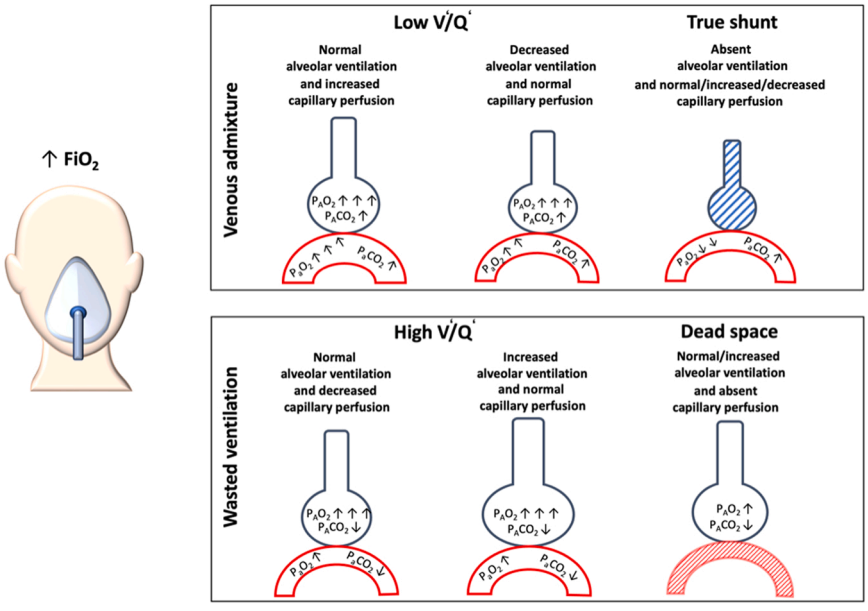

Fig. 5. Changes in gas exchange according to ventilation perfusion after increasing FiO_2. This figure depicts changes in gas exchange according to ventilation (V')/perfusion (Q') alterations after increasing the fraction of inspired oxygen (FiO_2). Above, venous admixture with three possible conditions: 1) low V'/Q' with normal alveolar ventilation and increased capillary perfusion that rising FiO_2 will determine marked increase of PaO_2 and P_AO_2; 2) low V'/Q' with decreased alveolar ventilation and normal capillary perfusion that rising FiO_2 will determine increase of PaO_2 and marked increase of P_AO_2; and 3) true shunt with absent alveolar ventilation and variable capillary perfusion not modified by FiO_2. Below, wasted ventilation with three possible conditions: 1) high V'/Q' with normal alveolar ventilation and decreased capillary perfusion that rising FiO_2 will determine marked increase of P_AO_2; 2) high V'/Q' with normal capillary perfusion that rising FiO_2 will determine marked increase of P_AO_2, and 3) dead space with normal alveolar ventilation but absent capillary perfusion that with FiO_2 will not change.

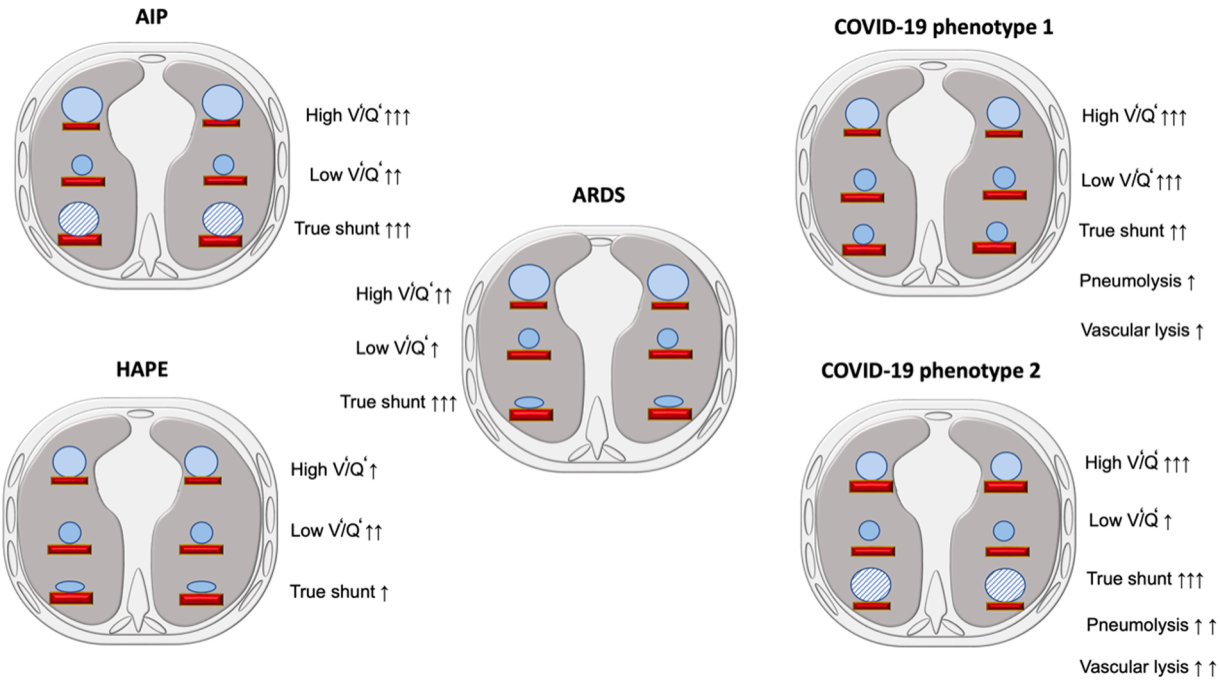

Fig. 6. Ventilation/ perfusion alteration in AIP, ARDS, HAPE, and COVID-19. This figure depicts ventilation (V')/ perfusion (Q') changes in five possible conditions. 1) AIP characterized mainly by wasted ventilation and true shunt due to alveolar consolidation with less low V'/Q'; 2) ARDS characterized mainly by mainly wasted ventilation and less low V'/Q', with high true shunt due to alveolar collapse, and the perfusion follow a gravitational gradient; 3) HEPA characterized by wasted ventilation and less low V'/Q', with high true shunt due to alveolar collapse; 4) COVID-19 phenotype 1 characterized by wasted ventilation and low V'/Q' and less true shunt due to alveolar consolidation but perfusion follow an antigravitational gradient; and 5) COVID-19 phenotype 2 characterized by wasted ventilation and low V'/Q' and higher true shunt mainly due to consolidation, and the perfusion follow an antigravitational gradient.

clinical diagnosis of HAPE is based on the presence of breathlessness, cough, chest discomfort and headache along with tachycardia, tachypnea, and a $SpO_2 < 86\%$ for an altitude of 3500 m in a patient arriving to high altitude within up to 5 days. (Chawla and Tripathi, 2015). Regarding gas exchange and ventilation distribution, HAPE presents mainly wasted ventilation and less low V/Q and high true shunt due to alveolar collapse (Fig. 6).

4.4. COVID-19 pneumonia

Patients with COVID-19 pneumonia may present "silent hypoxemia" or "asymptomatic hypoxemia" with a peripheral saturation of oxygen (SpO_2) < 95% at sea level (SpO_2 <85% at 3600 m), accompanied by shortness of breath upon mild exercise, fever, tachycardia, tachypnea, hyperventilation, with intercostal and diaphragmatic fatigue, the sensation of drowning, gasping and subsequent death. SARS-CoV-2 infection affects not only the lung (Zubieta-Calleja et al., 2021) but also other organs (Robba et al., 2020b). Clinical diagnosis is based on the presence of $SpO_2 < 90\%$ (PaO_2 <60 mmHg) at sea level and lower as altitude increases. In COVID-19, gas exchange is determined by the evolutive stages of the disease. In phenotype 1, lung weight is minimally increased compared to normal lungs (1.100 gr vs 800 gr, respectively), and hypoxemia is mainly associated with increased ground-glass regions and low V/Q areas are inhomogeneously distributed within the lung parenchyma. Low V/Q areas might be associated with lower ventilation and possibly some degree of hypoxic vasoconstriction and/or greater perfusion in normally and/or poorly aerated areas. The areas of low V'/Q' are markedly increased all over the lung from ventral to dorsal and from cranial to caudal lung regions (Pelosi et al., 1994) (Fig. 6). A possible explanation could be a decreased ventilatory drive, that may contribute to the silent hypoxemia. On the other hand, increased wasted ventilation due to the combination of high alveolar dead space and low V'/Q' is present in up to 40–50% of the total lung tissue mass, mainly due to diversion of ventilation toward non-dependent aerated lung regions and reduction in pulmonary perfusion due to increased airway pressure, collapse of capillaries and/or micro-thrombosis and formation of no recruitable atelectasis (Pelosi et al., 1994). This can also be justified by the increase in mucinous filling and pulmonary and vascular alterations (Ball et al., 2021c). In phenotype 2, lung weight is markedly increased (1600 −1700 gr), and hypoxemia is mainly associated with increased consolidated and non-aerated lung regions mainly distributed in the dependent lung regions. Under these clinical conditions, areas with low V'/Q' persist but also combined with areas of "true shunt". On the other hand, the amount of increased wasted ventilation is high and comparable with what is observed in phenotype 1 (L) (Fig. 6).

5. Intensive care management

All these four pathophysiological entities present similar but also peculiar characteristics of treatment. There is not specific treatment for AIP and ARDS being the management of these two conditions is mainly supportive (Tasaka et al., 2022; Xaubet et al., 2013). In AIP and ARDS of infective etiology, broad-spectrum antibiotics are recommended initially until infectious etiology is confirmed, thereby selecting narrower spectrum antibiotics. No clear benefit of corticosteroids has been confirmed in both AIP and ARDS (Chang et al., 2022). However, recent data suggest potential benefits of dexamethasone (Villar et al., 2020) or methylprednisolone and hydrocortisone in patients with ARDS (Chang et al., 2022). Further trials are warranted to confirm their efficacy. Supportive therapies for AIP are like those applied for ARDS, using a stepwise approach to increase the complexity of treatment according to the increased severity of lung disease. In mechanically ventilated subjects, a lung protective ventilator strategy should be adopted (Tasaka et al., 2022; Xaubet et al., 2013). In HAPE, the first-line treatment is the administration of oxygen and the rapid descent to lower altitudes. Medical therapy includes nifedine, whereas a phosphodiesterase type 5 inhibitor may be helpful but is not formally included in guidelines. Diuretics are not recommended (Wilkins et al., 2015). Treatment possibilities of COVID-19 pneumonia should consider both

anatomopathological and clinical findings. The separation in different phenotypes according to respiratory compliance has been recently challenged, concluding that no change in conventional lung-protective ventilation strategies is warranted (Reddy et al., 2022). We interpreted different phenotypes as an evolution and progression of the disease and lung injury and not as separate entities. In case of "silent hypoxemia", in which the degree of hypoxemia may not correspond to the severity of lung images and histopathological findings, early therapy may include the use of high-flow nasal oxygen or continuous positive end-expiratory pressure (CPAP) (Robba et al., 2021a). Noninvasive respiratory support can be considered as the first step toward COVID-19 management in phenotype 1, while early intubation and invasive mechanical ventilation should be considered for phenotype 2 or worsening of phenotype 1. A recent meta-analysis concluded that the timing of intubation may have no effect on mortality and morbidity in critically ill COVID-19 (Papoutsi et al., 2021). During invasive mechanical ventilation, COVID-19 patients showed a decrease in pulmonary and gas volume and increased regions of poorly aerated and non-aerated lung tissue more than patients treated with non-invasive respiratory support (Ball et al., 2021b). In COVID-19 phenotype-1 (L), a relatively preserved lung compliance is present with few areas that can be recruited and low V'/Q' areas. In this case, using a moderate PEEP level to redistribute pulmonary blood flow from non-ventilated to more ventilated areas could be suggested. Phenotype 2 (H) might benefit from invasive mechanical ventilation when non-invasive respiratory treatment is not effective, with progressive oxygen deterioration, prompt intubation is required. The respiratory treatment suggested is like that reported in "primary" ARDS with protective ventilation and moderate levels of PEEP individualized on patients' need, with cautious use of recruitment maneuvers. Prone position may be effective to improve oxygenation, but improvement in oxygenation is often associated with redistribution of perfusion and not effective alveolar recruitment (Rossi et al., 2021). Indeed, when the ventilation of dependent areas is impaired in the supine position, prone rescue positioning can be applied. The gravitational effect makes the dependent lungs areas more perfused following V'/Q' mismatch, thus resulting in hypoxemia, while prone position allows a more homogeneous distribution of ventilation and perfusion, reducing the risk of ventilator-induced lung injury (VILI), but improvement in oxygenation is often associated with redistribution of perfusion and not effective alveolar recruitment in COVID-19 (Battaglini et al., 2021; Rossi et al., 2021). The amount of consolidated tissue was higher in patients assessed during the third week and determined the oxygenation responses following pronation and recruitment maneuvers. In most refractory and severe cases, extracorporeal carbon dioxide removal (ECCO2R) and extracorporeal membrane oxygenation (ECMO) could be used in order to reduce Plateau pressures and tidal volumes and prevent VILI while adequately oxygenating the lungs and improving oxygen supply to all tissues (Battaglini et al., 2021). Other treatment options for improving gas exchange, include the use of erythropoietin in the treatment of severe COVID-19 pneumonia (Ehrenreich et al., 2020; Soliz et al., 2020) which can help improve the oxygen transport to tissues of the compromised oxygen transport triad (pneumo-dynamic pump, hemodynamic pump, and hemoglobin) (Zubieta-Calleja et al., 2021; Zubieta-Calleja and Zubieta-DeUrioste, 2021a). Erythropoietin could also exert indirect effects not limited to the increase of red blood cells, hematocrit and hemoglobin but also to the protective effects of the hormone in different tissues like the heart, the vessels, and the brain (Ehrenreich et al., 2020; Hadadi et al., 2020; Sahebnasagh et al., 2020). In fact, a correlation between acute lung injury and brain hypoxia has been described (Battaglini et al., 2020a). Hence, reduced systemic oxygenation can be associated with reduced brain tissue oxygenation and poor outcome (Battaglini et al., 2020a). Furthermore, the increase of hemoglobin becomes a fundamental factor of hypoxia tolerance, as previously shown by the Formula of Tolerance to hypoxia = $Hb/PaCO_2$ * 3.01 (Hb, hemoglobin; $PaCO_2$, arterial partial pressure of CO_2). This formula states that higher hemoglobin and a lower $PaCO_2$ give greater tolerance to hypoxia (Zubieta-Calleja et al., 2013). Indeed, PaO_2 and oxygen delivery (DO_2) can be optimized by modulating Hb concentration, pHa, $PaCO_2$, cardiac output, and arterial content of oxygen. Thus, increasing hemoglobin and cardiac output could be considered in this specific clinical setting in order to improve oxygen delivery (Battaglini et al., 2020a). In addition to these parameters, others should be considered when facing hypoxia at high altitude. According to the alveolar gas equation, the alveolar partial pressure of oxygen is dramatically decreased at high altitude, but a higher diffusion capacity is presumed, with a supposed physiological adaptation to altitude (Zubieta-Calleja et al., 2013). Some literature suggests that physiological adaptation to altitude may counterbalance the hypoxic environment thus protecting from severe SARS-CoV-2 infection, probably mediated by reduced survival of the virus at high altitude, and down-regulation of ACE2 (Arias-Reyes et al., 2020). Modulation of the inflammatory response is a matter of debate in both ARDS and COVID-19 (Chaudhuri et al., 2021). COVID-19 can trigger a "cytokines storm" in lung tissues and systemic circulation with the hyperactivation of the inflammatory-immune system. The accumulation of immune cells at infected sites can result in ARDS. Accordingly, a "cytokines storm" has been previously described in several conditions, including AIP and ARDS (Sinha et al., 2020). In HAPE, hyperinflammatory status has been attributed to the formation of pulmonary edema. The possible implication for treatment could be the recognition of those patients at higher risk of hyperinflammatory response to recognize hyper/ hypo-inflammatory sub-phenotypes such as those currently under investigation in ARDS. This is matter of debate since HAPE is a poorly defined pathophysiological entity, hence not clearly supporting the use of this terminology and its implication for therapy to date (Sinha et al., 2020). A universal agreement on the use of corticosteroids in non-COVID ARDS is still lacking, but national guidelines started to consider the use of low-dose steroids in ARDS, while recommending against the use of high doses that may result in immune suppression and increased risk of opportunistic infections (Tasaka et al., 2022). COVID-19 has boosted the pharmacological research investigating the role of several immunomodulating agents in respiratory failure, including steroids, anti-interleukin monoclonal antibodies and drugs with indirect action on the immune response (Battaglini et al., 2022). While the use of steroids in hospitalized COVID-19 patients requiring oxygen supplementation is an established practice, these are typically contraindicated in initial, mild COVID-19. The use of other immunomodulating agents requires careful patient selection in COVID-19 and, more importantly, caution when translating to ARDS the findings of studies conducted in COVID-19 related respiratory failure (Battaglini et al., 2022).

6. Potential overlap of pathways involved

6.1. *Renin-angiotensin system*

The renin-angiotensin system (RAS) has been identified as potential effector in the pathophysiology of pulmonary diseases. Particularly, angiotensin II exerts multiple function for maintaining the homeostasis of blood pressure, vasoconstriction, and sodium balance. Angiotensin converting enzyme2 (ACE2) also plays an important role. In fact ACE deficient mice or the use of inhibitors led to remodeling of pulmonary arterioles (Kuba et al., 2006) and Deletion/Deletion (D/D) polymorphism of ACE gene was associated with more severity of pulmonary symptoms (Kuba et al., 2006). ACE inhibitors may attenuate endothelial dysfunction and fibrosis in interstitial pneumonia. Both clinical and experimental animal studies have implicated ACE in the pathogenesis of ARDS (Marshall et al., 2002; Raiden et al., 2002), suggesting its role on pulmonary vascular tone/permeability, epithelial cell survival, and fibroblast activation. D/D gene polymorphism again was more abundant in patients with ARDS than general ICU/ general population, and was associated with higher mortality (Marshall et al., 2002). Recombinant ACE2 protein improved the symptoms and fibrotic changes in ARDS,

playing a protective role (Kuba et al., 2006). Similarly, HAPE recognizes the role of ACE2 and RAS in the pathogenesis of increased arterial pulmonary pressure, as occurs in response to hypoxia (Kleinsasser et al., 2012). The importance of the RAS in lung diseases has recently re-emerged with the identification of ACE2 in SARS-CoV-2. SARS-CoV-2 enters lung cells via the ACE2 receptor. ACE2 receptors are recognized by macrophages and other pro-inflammatory cells, spreading to other organs and infecting ACE2-expressing cells at local sites, potentially causing multi-organ disease (Al-Kuraishy et al., 2020).

6.2. Neuropilin-1

Neuropilin-1 (NPN-1) is a cell surface receptor that binds vascular endothelial growth factor (VEGF), potentially influencing endothelial permeability, chemotaxis, and proliferation. Inhibition of NPN-1 revealed attenuation of VEGF-mediated permeability of pulmonary artery endothelial cells, probably regulating endothelial barrier dysfunction in response to VEGF (Becker et al., 2005). In patients with ARDS, VEGF receptors 1 and 2 are up-regulated, whereas NPN-1 is down-regulated in comparison with patients without ARDS (Medford et al., 2009). Some studies demonstrated that changes in the plasma level of VEGF and soluble VEGF receptor-1 as well as NPN-1 are associated with HAPE (Zhang et al., 2018). In COVID-19, NPN-1 protein interacts with the host cell receptor is the Spike-1 (S1) subunit of the coronavirus, thus favoring SARS-CoV-2 entry into the cells, and in particular to the central nervous system (Al-kuraishy et al., 2021).

6.3. Hypoxia-inducible factor

Hypoxia-inducible factor (HIF)− 1 is a transcriptional activator dependent on oxygen, which plays an important role in maintaining oxygen homeostasis by regulating the expression of genes associated with adaptation to hypoxia. HIF-1 induces the release of inflammatory factors, thus exacerbating lung injury (Liu et al., 2020). During hypoxic conditions, HIF-1 induces VEGF expression regulating pulmonary vascular permeability and promotes alveolar type II cells apoptosis. In the progression of ARDS, HIF-1 enhances glucose metabolism in epithelial cells, thus increasing lung ventilation and improving pulmonary edema and respiratory distress (Liu et al., 2020). During normoxia, HIF-1α levels were recognized as markers of HAPE susceptibility (Soree et al., 2016). In COVID-19, HIF-1α promoted SARS-CoV-2 infection and aggravated inflammatory responses (Tian et al., 2021).

7. Future directions

COVID-19 may be complicated by the so called post-COVID-19 syndrome which manifests with symptoms duration for more than 3 months and progressive pulmonary fibrosis (Mehta et al., 2022). The pathogenesis of post-COVID-19 syndrome include direct tissue injury associated with autoimmunity antibodies. This new entity probably results from the interplay between epithelial and endothelial injury, immune-genetic susceptibility, ARDS, and/or ventilator-induced lung injury, hyperinflammation, and hypercoagulability, that in turn activate pro-fibrotic processes and a fibro-proliferative cascade. The impact of post-COVID-19 syndrome is currently unknown, as well as the influence of new COVID-19 variants, vaccination, ventilatory setting, immunomodulation and inflammation on it. The identification of COVID-19 phenotypes, as well as the understanding of physiological, radiological, and anatomopathological implications, and their evolution are paramount for progressing therapeutic targets and personalized medicine (Mehta et al., 2022).

8. Conclusions

Remodeling and destruction of lung tissue may explain silent hypoxemia, intubation ineffectiveness, rapid progression to severe gasping, and finally, death in most COVID-19 patients. These processes are characterized by active viral replication of COVID-19 within type-2 pneumocytes associated with persistent infiltration of inflammatory cells, as well as a continuous repair process, but with an intense reactive fibrotic activity and superimposed opportunistic infections that finally lead to death. For this reason, extensive destruction of the lung parenchyma can be easily confounded with other diseases that may coexist in COVID-19 but can also help to explain the post-disease fibrosis, residual respiratory insufficiency, and exercise limitation.

Ethics approval and consent to participate

Not applicable.

Consent for publication

Not applicable.

Funding

None.

CRediT authorship contribution statement

Gustavo R. Zubieta-Calleja: Writing – original draft, Conceptualization, Methodology, Visualization. **Natalia Zubieta-DeUrioste**: Writing – review & editing, Methodology. **Felipe de Jesús Montelongo**: Biopsies, Pathological photomicrographs, Writing pathological findings. **Manuel Gabriel Romo Sanchez**: Pathology preparation, Photomicrographs and writing pathological findings. **Aurio Fajardo Campoverdi**: Writing and editing. **Denise Battaglini, Patricia Rieken Macedo Rocco**: Writing, Editing, Validation. **Lorenzo Ball**: Validation, Editing. **Paolo Pelosi**: Writing, Editing.

Competing interests

None.

Data availability

No data was used for the research described in the article.

Acknowledgments

We acknowledge the late Prof. Dr. Gustavo Zubieta-Castillo (Sr.), our mentor. We also thank Lucrecia DeUrioste and Rafaela Zubieta-DeUrioste for their collaboration and suggestions.

References

Ackermann, M., Verleden, S.E., Kuehnel, M., Haverich, A., Welte, T., Laenger, F., Vanstapel, A., Werlein, C., Stark, H., Tzankov, A., Li, W.W., Li, V.W., Mentzer, S.J., Jonigk, D., 2020. Pulmonary vascular endothelialitis, thrombosis, and angiogenesis in Covid-19. N. Engl. J. Med 383, 120–128. https://doi.org/10.1056/NEJMoa2015432.

Al-kuraishy, H.M., Al-Gareeb, A.I., Alzahrani, K.J., Cruz-Martins, N., Batiha, G.E.-S., 2021. The potential role of neopterin in Covid-19: a new perspective. Mol. Cell. Biochem. 476, 4161–4166. https://doi.org/10.1007/s11010-021-04232-z.

Al-Kuraishy, H.M., Hussein, N.R., Al-Naimi, M.S., Al-Buhaidily, A.K., Al-Gareeb, A.I., Lungnier, C., 2020. Renin–Angiotensin system and fibrinolytic pathway in COVID-19: One-way skepticism. Biomed. Biotechnol. Res. J. 4, 33–40. https://doi.org/10.4103/bbrj.bbrj_105_20.

Angeles Montero-Fernandez, M., Pardo-Garcia, R., 2021. Histopathology features of the lung in COVID-19 patients. Diagn. Histopathol. 27, 123–127. https://doi.org/10.1016/j.mpdhp.2020.11.009.

Arias-Reyes, C., Zubieta-DeUrioste, N., Poma-Machicao, L., Aliaga-Raduan, F., Carvajal-Rodriguez, F., Dutschmann, M., Schneider-Gasser, E.M., Zubieta-Calleja, G., Soliz, J., 2020. Does the pathogenesis of SARS-CoV-2 virus decrease at high-altitude. Respir. Physiol. Neurobiol. 277, 103443 https://doi.org/10.1016/j.resp.2020.103443.

Ball, L., Barisione, E., Mastracci, L., Campora, M., Costa, D., Robba, C., Battaglini, D., Micali, M., Costantino, F., Cittadini, G., Patroniti, N., Pelosi, P., Fiocca, R., Grillo, F.,

2021a. Extension of Collagen Deposition in COVID-19 Post Mortem Lung Samples and Computed Tomography Analysis Findings. Int. J. Mol. Sci. 22, 7498. https://doi.org/10.3390/ijms22147498.

Ball, L., Robba, C., Maiello, L., Herrmann, J., Gerard, S.E., Xin, Y., Battaglini, D., Brunetti, I., Minetti, G., Seitun, S., Vena, A., Giacobbe, D.R., Bassetti, M., Rocco, P.R. M., Cereda, M., Castellan, L., Patroniti, N., Pelosi, P., Ball, L., Gratarola, A., Loconte, M., Molin, A., Orefice, G., Iannuzzi, F., Costantino, F., Battioni, D., Bovio, G., Buconte, G., Casaleggio, A., Cittadini, G., Dogliotti, L., Giasotto, V., Pigati, M., Santacroce, E., Zaottini, F., Dentone, C., Taramasso, L., Magnasco, L., Valbusa, A., Bastianello, M., 2021c. Computed tomography assessment of PEEP-induced alveolar recruitment in patients with severe COVID-19 pneumonia. Crit. Care 25, 81. https://doi.org/10.1186/s13054-021-03477-w.

Ball, L., Robba, C., Herrmann, J., Gerard, S.E., Xin, Y., Mandelli, M., Battaglini, D., Brunetti, I., Minetti, G., Seitun, S., Bovio, G., Vena, A., Giacobbe, D.R., Bassetti, M., Rocco, P.R.M., Cereda, M., Rizi, R.R., Castellan, L., Patroniti, N., Pelosi, P., Bixio, M., Gratarola, A., Frisoni, P., Loconte, M., Molin, A., Orefice, G., Ciaravolo, E., Costantino, F., Battioni, D., Buconte, G., Casaleggio, A., Cittadini, G., Dogliotti, L., Giasotto, V., Perissi, S., Pigati, M., Santacroce, E., Zaottini, F., Dentone, C., Taramasso, L., Magnasco, L., Bastianello, M., 2021b. Lung distribution of gas and blood volume in critically ill COVID-19 patients: a quantitative dual-energy computed tomography study. Crit. Care 25, 214. https://doi.org/10.1186/s13054-021-03610-9.

Barisione, E., Grillo, F., Ball, L., Bianchi, R., Grosso, M., Morbini, P., Pelosi, P., Patroniti, N.A., De Lucia, A., Orengo, G., Gratarola, A., Verda, M., Cittadini, G., Mastracci, L., Fiocca, R., 2020. Fibrotic progression and radiologic correlation in matched lung samples from COVID-19 post-mortems. Virchows Arch. 1–15. https://doi.org/10.1007/s00428-020-02934-1.

Barisione, E., Grillo, F., Ball, L., Bianchi, R., Grosso, M., Morbini, P., Pelosi, P., Patroniti, N.A., De Lucia, A., Orengo, G., Gratarola, A., Verda, M., Cittadini, G., Mastracci, L., Fiocca, R., 2021. Fibrotic progression and radiologic correlation in matched lung samples from COVID-19 post-mortems. Virchows Arch. 478, 471–485. https://doi.org/10.1007/s00428-020-02934-1.

Barton, L.M., Duval, E.J., Stroberg, E., Ghosh, S., Mukhopadhyay, S., 2020. COVID-19 Autopsies, Oklahoma, USA. Am. J. Clin. Pathol. 153, 725–733. https://doi.org/10.1093/ajcp/aqaa062.

Batah, S.S., Fabro, A.T., 2021. Pulmonary pathology of ARDS in COVID-19: A pathological review for clinicians. Respir. Med. 176, 106239 https://doi.org/10.1016/j.rmed.2020.106239.

Battaglini, D., Cruz, F., Robba, C., Pelosi, P., Rocco, P.R.M., 2022. Failed clinical trials on COVID-19 acute respiratory distress syndrome in hospitalized patients: common oversights and streamlining the development of clinically effective therapeutics. Expert Opin. Investig. Drugs. https://doi.org/10.1080/13543784.2022.2120801.

Battaglini, D., Sottano, M., Ball, L., Robba, C., Rocco, P.R.M., Pelosi, P., 2021. Ten golden rules for individualized mechanical ventilation in acute respiratory distress syndrome. J. Intensive Med 1, 42–51. https://doi.org/10.1016/j.jointm.2021.01.003.

Battaglini, D., Brunetti, I., Anania, P., Fiaschi, P., Zona, G., Ball, L., Giacobbe, D.R., Vena, A., Bassetti, M., Patroniti, N., Schenone, A., Pelosi, P., Rocco, P.R.M., Robba, C., 2020a. Neurological Manifestations of Severe SARS-CoV-2 Infection: Potential Mechanisms and Implications of Individualized Mechanical Ventilation Settings. Front. Neurol. 11, 845. https://doi.org/10.3389/fneur.2020.00845.

Battaglini, D., Santori, G., Chandraptham, K., Iannuzzi, F., Bastianello, M., Tarantino, F., Ball, L., Giacobbe, D.R., Vena, A., Bassetti, M., Inglese, M., Uccelli, A., Rocco, P.R.M., Patroniti, N., Brunetti, I., Pelosi, P., Robba, C., 2020b. Neurological Complications and Noninvasive Multimodal Neuromonitoring in Critically Ill Mechanically Ventilated COVID-19 Patients. Front. Neurol. 11, 602114 https://doi.org/10.3389/fneur.2020.602114.

Becker, P.M., Waltenberger, J., Yachechko, R., Mirzapoiazova, T., Sham, J.S.K., Lee, C. G., Elias, J.A., Verin, A.D., 2005. Neuropilin-1 Regulates Vascular Endothelial Growth Factor–Mediated Endothelial Permeability. Circ. Res. 96, 1257–1265. https://doi.org/10.1161/01.RES.0000171756.13554.49.

Cardinal-Fernández, P., Lorente, J.A., Ballén-Barragán, A., Matute-Bello, G., 2017. Acute respiratory distress syndrome and diffuse alveolar damage. New insights on a complex relationship. Ann. Am. Thorac. Soc. 14, 844–850. https://doi.org/10.1513/AnnalsATS.201609-728PS.

Chanana, N., Palmo, T., Newman, J.H., Pasha, M.A.Q., 2020. Vascular homeostasis at high-altitude: role of genetic variants and transcription factors. Pulm. Circ. 10 https://doi.org/10.1177/2045894020913475.

Chang, X., Li, S., Fu, Y., Dang, H., Liu, C., 2022. Safety and efficacy of corticosteroids in ARDS patients: a systematic review and meta-analysis of RCT data. Respir. Res. 23, 301. https://doi.org/10.1186/s12931-022-02186-4.

Chaudhuri, D., Sasaki, K., Karkar, A., Sharif, S., Lewis, K., Mammen, M.J., Alexander, P., Ye, Z., Lozano, L.E.C., Munch, M.W., Perner, A., Du, B., Mbuagbaw, L., Alhazzani, W., Pastores, S.M., Marshall, J., Lamontagne, F., Annane, D., Meduri, G. U., Rochwerg, B., 2021. Corticosteroids in COVID-19 and non-COVID-19 ARDS: a systematic review and meta-analysis. Intensive Care Med 47, 521–537. https://doi.org/10.1007/s00134-021-06394-2.

Chawla, A., Tripathi, K.K., 2015. Objective criteria for diagnosing high altitude pulmonary edema in acclimatized patients at altitudes between 2700m and 3500m. Med. J. Armed Forces India 71, 345–351. https://doi.org/10.1016/j.mjafi.2015.09.002.

Dakin, J., Jones, A.T., Hansell, D.M., Hoffman, E.A., Evans, T.W., 2011. Changes in lung composition and regional perfusion and tissue distribution in patients with ARDS. Respirology 16, 1265–1272. https://doi.org/10.1111/j.1440-1843.2011.02048.x.

De Marzo, V., Di Biagio, A., Della Bona, R., Vena, A., Arboscello, E., Emirjona, H., Mora, S., Giacomini, M., Da Rin, G., Pelosi, P., Bassetti, M., Ameri, P., Porto, I., 2021. Prevalence and prognostic value of cardiac troponin in elderly patients hospitalized for COVID-19. J. Geriatr. Cardiol. 18, 338–345. https://doi.org/10.11909/j.issn.1671-5411.2021.05.004.

Dehnert, C., Risse, F., Ley, S., Kuder, T.A., Buhmann, R., Puderbach, M., Menold, E., Mereles, D., Kauczor, H.-U., Bärtsch, P., Fink, C., 2006. Magnetic Resonance Imaging of Uneven Pulmonary Perfusion in Hypoxia in Humans. Am. J. Respir. Crit. Care Med 174, 1132–1138. https://doi.org/10.1164/rccm.200606-780OC.

Desai, S.R., Wells, A.U., Rubens, M.B., Evans, T.W., Hansell, D.M., 1999. Acute Respiratory Distress Syndrome: CT Abnormalities at Long-term Follow-up. Radiology 210, 29–35. https://doi.org/10.1148/radiology.210.1.r99ja2629.

Droma, Y., Hanaoka, M., Hotta, J., Naramoto, A., Koizumi, T., Fujimoto, K., Honda, T., Kobayashi, T., Kubo, K., 2001. Pathological features of the lung in fatal high altitude pulmonary edema occurring at moderate altitude in Japan. High. Alt. Med. Biol. 2, 515–523. https://doi.org/10.1089/152702901753397081.

Edler, C., Schröder, A.S., Aepfelbacher, M., Fitzek, A., Heinemann, A., Heinrich, F., Klein, A., Langenwalder, F., Lütgehetmann, M., Meißner, K., Püschel, K., Schädler, J., Steurer, S., Mushumba, H., Sperhake, J.-P., 2020. Dying with SARS-CoV-2 infection—an autopsy study of the first consecutive 80 cases in Hamburg, Germany. Int. J. Leg. Med 134, 1275–1284. https://doi.org/10.1007/s00414-020-02317-w.

Ehrenreich, H., Weissenborn, K., Begemann, M., Busch, M., Vieta, E., Miskowiak, K.W., 2020. Erythropoietin as candidate for supportive treatment of severe COVID-19. Mol. Med. 26, 58. https://doi.org/10.1186/s10020-020-00186-y.

Fajardo, A., Medina, A., Modesto, V., Gordo-Vidal, F., 2020. El lado oculto de la hipoxemia. Rev. Chil. Anest. 49, 784–794. https://doi.org/10.25237/revchilanestv49n06-4.

Ferreira, J.C., Ho, Y.L., Adler Maccagnan, B., Besen, P., Sa Malbouisson, L.M., Utino Taniguchi, L., Vitale Mendes, P., Leite Vieira Costa, E., Park, M., Daltro-Oliveira, R., Roepke, M.L., R., M, Silva-Jr, J., Carvalho Carmona, M.J., Carvalho, C.R.R., on behalf of EPICCoV Study Group, 2021. Protective ventilation and outcomes of critically ill patients with COVID-19: a cohort study. Ann. Intensive Care 11, 92. https://doi.org/10.1186/s13613-021-00882-w.

Garrido, E., Maglia, J.B., de, Sibila, O., Zubieta-Calleja, G., 2022. High-altitude pulmonary edema in the context of COVID-19. OBM Genet 6, 1. https://doi.org/10.21926/obm.genet.2203163.

Gattinoni, L., Caironi, P., Pelosi, P., Goodman, L.R., 2001. What has computed tomography taught us about the acute respiratory distress syndrome? Am. J. Respir. Crit. Care Med 164, 1701–1711. https://doi.org/10.1164/ajrccm.164.9.2103121.

Gattinoni, L., Bombino, M., Pelosi, P., Lissoni, A., Pesenti, A., Fumagalli, R., Tagliabue, M., 1994. Lung structure and function in different stages of severe adult respiratory distress syndrome. JAMA 271, 1772–1779.

Gattinoni, L., Chiumello, D., Caironi, P., Busana, M., Romitti, F., Brazzi, L., Camporota, L., 2020. COVID-19 pneumonia: different respiratory treatments for different phenotypes. Intensive Care Med 46, 1099–1102. https://doi.org/10.1007/s00134-020-06033-2.

Giesenhagen, A.M., Ivy, D.D., Brinton, J.T., Meier, M.R., Weinman, J.P., Liptzin, D.R., 2019. High altitude pulmonary edema in children: a single referral center evaluation. J. Pedia 210, 106–111. https://doi.org/10.1016/j.jpeds.2019.02.028.

Goodman, L.R., Fumagalli, R., Tagliabue, P., Tagliabue, M., Ferrario, M., Gattinoni, L., Pesenti, A., 1999. Adult Respiratory Distress Syndrome Due to Pulmonary and Extrapulmonary Causes: CT, Clinical, and Functional Correlations. Radiology 213, 545–552. https://doi.org/10.1148/radiology.213.2.r99nv42545.

Guerin, C., Bayle, F., Leray, V., Debord, S., Stoian, A., Yonis, H., Roudaut, J.-B., Bourdin, G., Devouassoux-Shisheboran, M., Bucher, E., Ayzac, L., Lantuejoul, S., Philipponnet, C., Kemeny, J.L., Souweine, B., Richard, J.-C., 2015. Open lung biopsy in nonresolving ARDS frequently identifies diffuse alveolar damage regardless of the severity stage and may have implications for patient management. Intensive Care Med 41, 222–230. https://doi.org/10.1007/s00134-014-3583-2.

Hadadi, A., Mortezazadeh, M., Kolahdouzan, K., Alavian, G., 2020. Does recombinant human erythropoietin administration in critically ill COVID-19 patients have miraculous therapeutic effects. ? J. Med. Virol. 92, 915–918. https://doi.org/10.1002/jmv.25839.

Hall, L.F., 1938. Pneumolysis in the treatment of pulmonary tuberculosis. Dis. Chest 4, 18–20. https://doi.org/10.1378/chest.4.11.18.

Hanley, B., Lucas, S.B., Youd, E., Swift, B., Osborn, M., 2020. Autopsy in suspected COVID-19 cases. J. Clin. Pathol. 73, 239–242. https://doi.org/10.1136/jclinpath-2020-206522.

Hellman, U., Karlsson, M.G., Engström-Laurent, A., Cajander, S., Dorofte, L., Ahlm, C., Laurent, C., Blomberg, A., 2020. Presence of hyaluronan in lung alveoli in severe Covid-19: An opening for new treatment options. ? J. Biol. Chem. 295, 15418–15422. https://doi.org/10.1074/jbc.AC120.015967.

Hopkins, S.R., Garg, J., Bolar, D.S., Balouch, J., Levin, D.L., 2005. Pulmonary blood flow heterogeneity during hypoxia and high-altitude pulmonary edema. Am. J. Respir. Crit. Care Med 171, 83–87. https://doi.org/10.1164/rccm.200406-707OC.

Huertas, A., Guignabert, C., Barberà, J.A., Bärtsch, P., Bhattacharya, J., Bhattacharya, S., Bonsignore, M.R., Dewachter, L., Dinh-Xuan, A.T., Dorfmüller, P., Gladwin, M.T., Humbert, M., Kotsimbos, T., Vassilakopoulos, T., Sanchez, O., Savale, L., Testa, U., Wilkins, M.R., 2018. Pulmonary vascular endothelium: the orchestra conductor in respiratory diseases. Eur. Respir. J. 51, 1700745. https://doi.org/10.1183/13993003.00745-2017.

Kamp, J.C., Neubert, L., Ackermann, M., Stark, H., Werlein, C., Fuge, J., Haverich, A., Tzankov, A., Steinestel, K., Friemann, J., Boor, P., Junker, K., Hoeper, M.M., Welte, T., Laenger, F., Kuehnel, M.P., Jonigk, D.D., 2022. Time-Dependent Molecular Motifs of Pulmonary Fibrogenesis in COVID-19. Int. J. Mol. Sci. 23, 1583. https://doi.org/10.3390/ijms23031583.

Karbing, D.S., Panigada, M., Bottino, N., Spinelli, E., Protti, A., Rees, S.E., Gattinoni, L., 2020. Changes in shunt, ventilation/perfusion mismatch, and lung aeration with

PEEP in patients with ARDS: a prospective single-arm interventional study. Crit. Care 24, 111. https://doi.org/10.1186/s13054-020-2834-6.
Kleinsasser, A., Pircher, I., Treml, B., Schwienbacher, M., Schuster, M., Janzek, E., Loibner, H., Penninger, J.M., Loeckinger, A., 2012. Recombinant Angiotensin-Converting Enzyme 2 Suppresses Pulmonary Vasoconstriction in Acute Hypoxia. Wilderness Environ. Med. 23, 24–30. https://doi.org/10.1016/j.wem.2011.09.002.
Kuba, K., Imai, Y., Penninger, J., 2006. Angiotensin-converting enzyme 2 in lung diseases. Curr. Opin. Pharmacol. 6, 271–276. https://doi.org/10.1016/j.coph.2006.03.001.
Lavinio, A., Ercole, A., Battaglini, D., Magnoni, S., Badenes, R., Taccone, F.S., Helbok, R., Thomas, W., Pelosi, P., Robba, C., 2021. Safety profile of enhanced thromboprophylaxis strategies for critically ill COVID-19 patients during the first wave of the pandemic: observational report from 28 European intensive care units. Crit. Care 25, 155. https://doi.org/10.1186/s13054-021-03543-3.
Lin, L., Lu, L., Cao, W., Li, T., 2020. Hypothesis for potential pathogenesis of SARS-CoV-2 infection–a review of immune changes in patients with viral pneumonia. Emerg. Microbes Infect. 9, 727–732. https://doi.org/10.1080/22221751.2020.1746199.
Liu, Y., Xiang, D., Zhang, H., Yao, H., Wang, Y., 2020. Hypoxia-Inducible Factor-1: A Potential Target to Treat Acute Lung Injury. Oxid. Med. Cell. Longev. 2020, 1–13. https://doi.org/10.1155/2020/8871476.
Lopes-Pacheco, M., Silva, P.L., Cruz, F.F., Battaglini, D., Robba, C., Pelosi, P., Morales, M. M., Caruso Neves, C., Rocco, P.R.M., 2021. Pathogenesis of Multiple Organ Injury in COVID-19 and Potential Therapeutic Strategies. Front. Physiol. 12, 593223 https://doi.org/10.3389/fphys.2021.593223.
Marshall, R.P., Webb, S., Bellingan, G.J., Montgomery, H.E., Chaudhari, B., McAnulty, R. J., Humphries, S.E., Hill, M.R., Laurent, G.J., 2002. Angiotensin converting enzyme insertion/deletion polymorphism is associated with susceptibility and outcome in acute respiratory distress syndrome. Am. J. Respir. Crit. Care Med 166, 646–650. https://doi.org/10.1164/rccm.2108086.
Medford, A.R.L., Ibrahim, N.B.N., Millar, A.B., 2009. Vascular endothelial growth factor receptor and coreceptor expression in human acute respiratory distress syndrome. J. Crit. Care 24, 236–242. https://doi.org/10.1016/j.jcrc.2008.04.003.
Mehta, P., Rosas, I.O., Singer, M., 2022. Understanding post-COVID-19 interstitial lung disease (ILD): a new fibroinflammatory disease entity. Intensive Care Med 1–4. https://doi.org/10.1007/s00134-022-06877-w.
Menezes, S.L.S., Bozza, P.T., Faria Neto, H.C.C., Laranjeira, A.P., Negri, E.M., Capelozzi, V.L., Zin, W.A., Rocco, P.R.M., 2005. Pulmonary and extrapulmonary acute lung injury: inflammatory and ultrastructural analyses. J. Appl. Physiol. 98, 1777–1783. https://doi.org/10.1152/japplphysiol.01182.2004.
Mitra, P., Misra, S., Sharma, P., 2020. COVID-19 pandemic in India: what lies ahead. Indian J. Clin. Biochem. 35, 257–259. https://doi.org/10.1007/s12291-020-00886-6.
Mukhopadhyay, S., Parambil, J., 2012. Acute Interstitial Pneumonia (AIP): Relationship to Hamman-Rich Syndrome, Diffuse Alveolar Damage (DAD), and Acute Respiratory Distress Syndrome (ARDS. Semin. Respir. Crit. Care Med. 33, 476–485. https://doi.org/10.1055/s-0032-1325158.
Nair, V., Singh, P., Yanamandra, U., Gupta, A., Grewal, R., Vardhan, V., Saxena, P., Mulajkar, D., 2021. Radiographical Spectrum of High-altitude Pulmonary Edema: A Pictorial Essay. Indian J. Crit. Care Med 25, 668–674. https://doi.org/10.5005/jp-journals-10071-23827.
Obadina, E.T., Torrealba, J.M., Kanne, J.P., 2013. Acute pulmonary injury: high-resolution CT and histopathological spectrum. Br. J. Radio. 86, 20120614. https://doi.org/10.1259/bjr.20120614.
Orlandi, D., Battaglini, D., Robba, C., Viganò, M., Bergamaschi, G., Mignatti, T., ML, R., Lapolla, A., Turtulici, G., Pelosi, P., 2021. COVID-19 phenotypes, lung ultrasound, chest computed tomography, and clinical features in critically ill mechanically ventilated patients. Ultrasound Med. Biol. 47, 3323–3332. https://doi.org/10.1016/j.ultrasmedbio.2021.07.014.
Palmucci, S., Roccasalva, F., Puglisi, S., Torrisi, S.E., Vindigni, V., Mauro, L.A., Ettorre, G. C., Piccoli, M., Vancheri, C., 2014. Clinical and radiological features of idiopathic interstitial pneumonias (IIPs): a pictorial review. Insights Imaging 5, 347–364. https://doi.org/10.1007/s13244-014-0335-3.
Papoutsi, E., Giannakoulis, V.G., Xourgia, E., Routsi, C., Kotanidou, A., Siempos, I.I., 2021. Effect of timing of intubation on clinical outcomes of critically ill patients with COVID-19: a systematic review and meta-analysis of non-randomized cohort studies. Crit. Care 25, 121. https://doi.org/10.1186/s13054-021-03540-6.
Pelosi, P., D'Andrea, L., Vitale, G., Pesenti, A., Gattinoni, L., 1994. Vertical gradient of regional lung inflation in adult respiratory distress syndrome. Am. J. Respir. Crit. Care Med 149, 8–13. https://doi.org/10.1164/ajrccm.149.1.8111603.
Pelosi, P., D'Onofrio, D., Chiumello, D., Paolo, S., Chiara, G., Capelozzi, V.L., Barbas, C.S. V., Chiaranda, M., Gattinoni, L., 2003. Pulmonary and extrapulmonary acute respiratory distress syndrome are different. Eur. Respir. J. 22, 48s–56s. https://doi.org/10.1183/09031936.03.00420803.
Petersson, J., Glenny, R.W., 2014. Gas exchange and ventilation–perfusion relationships in the lung. Eur. Respir. J. 44, 1023–1041. https://doi.org/10.1183/09031936.00037014.
Pomara, C., Li Volti, G., Cappello, F., 2020. COVID-19 Deaths: Are We Sure It Is Pneumonia? Please, Autopsy, Autopsy, Autopsy. ! J. Clin. Med 9, 1259. https://doi.org/10.3390/jcm9051259.
Primack, S.L., Hartman, T.E., Ikezoe, J., Akira, M., Sakatani, M., Müller, N.L., 1993. Acute interstitial pneumonia: radiographic and CT findings in nine patients. Radiology 188, 817–820. https://doi.org/10.1148/radiology.188.3.8351354.
Raiden, S., Nahmod, K., Nahmod, V., Semeniuk, G., Pereira, Y., Alvarez, C., Giordano, M., Geffner, J.R., 2002. Nonpeptide Antagonists of AT1 Receptor for Angiotensin II Delay the Onset of Acute Respiratory Distress Syndrome. J. Pharmacol. Exp. Ther. 303, 45–51. https://doi.org/10.1124/jpet.102.037382.
Ranieri, V., Rubenfeld, G., Thompson, B., Ferguson, N., Caldwell, E., Fan, E., Camporota, L., Slutsky, A., 2012. Acute Respiratory Distress Syndrome: the Berlin Definition. JAMA 307, 2526–2533. https://doi.org/10.1001/jama.2012.5669.
Reddy, M.P., Subramaniam, A., Chua, C., Ling, R.R., Anstey, C., Ramanathan, K., Slutsky, A.S., Shekar, K., 2022. Respiratory system mechanics, gas exchange, and outcomes in mechanically ventilated patients with COVID-19-related acute respiratory distress syndrome: a systematic review and meta-analysis. Lancet Respir. Med. https://doi.org/10.1016/S2213-2600(22)00393-9.
Robba, C., Battaglini, D., Pelosi, P., Rocco, P.R.M., 2020b. Multiple organ dysfunction in SARS-CoV-2: MODS-CoV-2. Expert Rev. Respir. Med. 14, 865–868. https://doi.org/10.1080/17476348.2020.1778470.
Robba, C., Battaglini, D., Ball, L., Pelosi, P., Rocco, P.R.M., 2021a. Ten things you need to know about intensive care unit management of mechanically ventilated patients with COVID-19. Expert Rev. Respir. Med 17476348 (2021), 1906226. https://doi.org/10.1080/17476348.2021.1906226.
Robba, C., Battaglini, D., Ball, L., Patroniti, N., Loconte, M., Brunetti, I., Vena, A., Giacobbe, D.R., Bassetti, M., Rocco, P.R.M., Pelosi, P., 2020a. Distinct phenotypes require distinct respiratory management strategies in severe COVID-19. Respir. Physiol. Neurobiol. 279, 103455 https://doi.org/10.1016/j.resp.2020.103455.
Robba, C., Battaglini, D., Ball, L., Valbusa, A., Porto, I., Della Bona, R., La Malfa, G., Patroniti, N., Brunetti, I., Loconte, M., Bassetti, M., Giacobbe, D.R., Vena, A., Silva, C.L.M., Rocco, P.R.M., Pelosi, P., 2021b. Coagulative Disorders in Critically Ill COVID-19 Patients with Acute Distress Respiratory Syndrome: A Critical Review. J. Clin. Med 10, 140. https://doi.org/10.3390/jcm10010140.
Rocco, P.R., Pelosi, P., 2008. Pulmonary and extrapulmonary acute respiratory distress syndrome: myth or reality? Curr. Opin. Crit. Care 14, 50–55. https://doi.org/10.1097/MCC.0b013e3282f2405b.
Rossi, S., Palumbo, M.M., Sverzellati, N., Busana, M., Malchiodi, L., Bresciani, P., Ceccarelli, P., Sani, E., Romitti, F., Bonifazi, M., Gattarello, S., Steinberg, I., Palermo, P., Lazzari, S., Collino, F., Cressoni, M., Herrmann, P., Saager, L., Meissner, K., Quintel, M., Camporota, L., Marini, J.J., Gattinoni, L., 2021. Mechanisms of oxygenation responses to proning and recruitment in COVID-19 pneumonia. Intensive Care Med 48, 1–11. https://doi.org/10.1007/s00134-021-06562-4.
Sahebnasagh, A., Mojtahedzadeh, M., Najmeddin, F., Najafi, A., Safdari, M., Rezai Ghaleno, H., Habtemariam, S., Berindan-Neagoe, I., Nabavi, S.M., 2020. A Perspective on Erythropoietin as a Potential Adjuvant Therapy for Acute Lung Injury/Acute Respiratory Distress Syndrome in Patients with COVID-19. Arch. Med. Res. 51, 631–635. https://doi.org/10.1016/j.arcmed.2020.08.002.
Sinha, P., Matthay, M.A., Calfee, C.S., 2020. Is a "Cytokine Storm" Relevant to COVID-19? JAMA. Intern. Med 180, 1152. https://doi.org/10.1001/jamainternmed.2020.3313.
Soliz, J., Schneider-Gasser, E.M., Arias-Reyes, C., Aliaga-Raduan, F., Poma-Machicao, L., Zubieta-Calleja, G., Furuya, W.I., Trevizan-Baú, P., Dhingra, R.R., Dutschmann, M., 2020. Coping with hypoxemia: Could erythropoietin (EPO) be an adjuvant treatment of COVID-19. Respir. Physiol. Neurobiol. 279, 103476 https://doi.org/10.1016/j.resp.2020.103476.
Soree, P., Gupta, R.K., Singh, K., Desiraju, K., Agrawal, A., Vats, P., Bharadwaj, A., Baburaj, T.P., Chaudhary, P., Singh, V.K., Verma, S., Bajaj, A.C., Singh, S.B., 2016. Raised HIF1α during normoxia in high altitude pulmonary edema susceptible non-mountaineers. Sci. Rep. 6, 26468. https://doi.org/10.1038/srep26468.
Suga, K., Kawakami, Y., Koike, M., Iwanaga, H., Matsunaga, N., 2009. Characteristic crescentic subpleural lung zones with high ventilation (V)/perfusion (Q) ratios in interstitial pneumonia on V/Q quotient SPECT. Nucl. Med. Commun. 30, 881–889. https://doi.org/10.1097/MNM.0b013e328330571d.
Tasaka, S., Ohshimo, S., Takeuchi, M., Yasuda, H., Ichikado, K., Tsushima, K., Egi, M., et al., 2022. ARDS clinical practice guideline 2021. J. Intensive Care 10, 32. https://doi.org/10.1186/s40560-022-00615-6.
Thille, A.W., Esteban, A., Fernández-Segoviano, P., Rodriguez, J.-M., Aramburu, J.-A., Peñuelas, O., Cortés-Puch, I., Cardinal-Fernández, P., Lorente, J.A., Frutos-Vivar, F., 2013. Comparison of the Berlin Definition for Acute Respiratory Distress Syndrome with Autopsy. Am. J. Respir. Crit. Care Med 187, 761–767. https://doi.org/10.1164/rccm.201211-1981OC.
Tian, M., Liu, W., Li, X., Zhao, P., Shereen, M.A., Zhu, C., Huang, S., Liu, S., Yu, X., Yue, M., Pan, P., Wang, W., Li, Y., Chen, X., Wu, K., Luo, Z., Zhang, Q., Wu, J., 2021. HIF-1α promotes SARS-CoV-2 infection and aggravates inflammatory responses to COVID-19. Signal Transduct. Target. Ther. 6, 308. https://doi.org/10.1038/s41392-021-00726-w.
Tonelli, R., Marchioni, A., Tabbì, L., Fantini, R., Busani, S., Castaniere, I., Andrisani, D., Gozzi, F., Bruzzi, G., Manicardi, L., Demurtas, J., Andreani, A., Cappiello, G.F., Samarelli, A.V., Clini, E., 2021. Spontaneous Breathing and Evolving Phenotypes of Lung Damage in Patients with COVID-19: Review of Current Evidence and Forecast of a New Scenario. J. Clin. Med 10, 975. https://doi.org/10.3390/jcm10050975.
Travis, W.D., Costabel, U., Hansell, D.M., King, T.E., Lynch, D.A., Nicholson, A.G., Ryerson, C.J., Ryu, J.H., Selman, M., Wells, A.U., Behr, J., Bouros, D., Brown, K.K., Colby, T.V., Collard, H.R., Cordeiro, C.R., Cottin, V., Crestani, B., Drent, M., Dudden, R.F., Egan, J., Flaherty, K., Hogaboam, C., Inoue, Y., Johkoh, T., Kim, D.S., Kitaichi, M., Loyd, J., Martinez, F.J., Myers, J., Protzko, S., Raghu, G., Richeldi, L., Sverzellati, N., Swigris, J., Valeyre, D., 2013. An Official American Thoracic Society/European Respiratory Society Statement: Update of the International Multidisciplinary Classification of the Idiopathic Interstitial Pneumonias. Am. J. Respir. Crit. Care Med 188, 733–748. https://doi.org/10.1164/rccm.201308-1483ST.
Villar, J., Ferrando, C., Martínez, D., Ambrós, A., Muñoz, T., Soler, J.A., Aguilar, G., Alba, F., González-Higueras, E., Conesa, L.A., Martín-Rodríguez, C., Díaz-Domínguez, F.J., Serna-Grande, P., Rivas, R., Ferreres, J., Belda, J., Capilla, L.,

Tallet, A., Añón, J.M., Fernández, R.L., González-Martín, J.M., Aguilar, G., Alba, F., Álvarez, J., Ambrós, A., Añón, J.M., Asensio, M.J., Belda, J., Blanco, J., Blasco, M., Cachafeiro, L., del Campo, R., Capilla, L., Carbonell, J.A., Carbonell, N., Cariñena, A., Carriedo, D., Chico, M., Conesa, L.A., Corpas, R., Cuervo, J., Díaz-Domínguez, F.J., Domínguez-Antelo, C., Fernández, L., Fernández, R.L., Ferrando, C., Ferreres, J., Gamboa, E., González-Higueras, E., González-Luengo, R.I., González-Martín, J.M., Martínez, D., Martín-Rodríguez, C., Muñoz, T., Ortiz Díaz-Miguel, R., Pérez-González, R., Prieto, A.M., Prieto, I., Rivas, R., Rojas-Viguera, L., Romera, M.A., Sánchez-Ballesteros, J., Segura, J.M., Serna-Grande, P., Serrano, A., Solano, R., Soler, J.A., Soro, M., Tallet, A., Villar, J., 2020. Dexamethasone treatment for the acute respiratory distress syndrome: a multicentre, randomised controlled trial. Lancet Respir. Med 8, 267–276. https://doi.org/10.1016/S2213-2600(19)30417-5.

Wichmann, D., Sperhake, J.-P., Lütgehetmann, M., Steurer, S., Edler, C., Heinemann, A., Heinrich, F., Mushumba, H., Kniep, I., Schröder, A.S., Burdelski, C., de Heer, G., Nierhaus, A., Frings, D., Pfefferle, S., Becker, H., Bredereke-Wiedling, H., de Weerth, A., Paschen, H.-R., Sheikhzadeh-Eggers, S., Stang, A., Schmiedel, S., Bokemeyer, C., Addo, M.M., Aepfelbacher, M., Püschel, K., Kluge, S., 2020. Autopsy findings and venous thromboembolism in patients with COVID-19. Ann. Intern. Med. 173, 268–277. https://doi.org/10.7326/M20-2003.

Wiersinga, W.J., Rhodes, A., Cheng, A.C., Peacock, S.J., Prescott, H.C., 2020. Pathophysiology, transmission, diagnosis, and treatment of Coronavirus Disease 2019 (COVID-19). JAMA 324, 782. https://doi.org/10.1001/jama.2020.12839.

Wilkins, M.R., Ghofrani, H.-A., Weissmann, N., Aldashev, A., Zhao, L., 2015. Pathophysiology and treatment of high-altitude pulmonary vascular disease. Circulation 131, 582–590. https://doi.org/10.1161/CIRCULATIONAHA.114.006977.

Xaubet, A., Ancochea, J., Bollo, E., Fernández-Fabrellas, E., Franquet, T., Molina-Molina, M., Montero, M.A., Serrano-Mollar, A., 2013. Guidelines for the Diagnosis and Treatment of Idiopathic Pulmonary Fibrosis. Arch. Bronconeumol. (Engl. Ed. 49, 343–353. https://doi.org/10.1016/j.arbr.2013.06.003.

Xu, Z., Shi, L., Wang, Y., Zhang, J., Huang, L., Zhang, C., Liu, S., Zhao, P., Liu, H., Zhu, L., Tai, Y., Bai, C., Gao, T., Song, J., Xia, P., Dong, J., Zhao, J., Wang, F.-S., 2020. Pathological findings of COVID-19 associated with acute respiratory distress syndrome. Lancet Respir. Med. 8, 420–422. https://doi.org/10.1016/S2213-2600(20)30076-X.

Yan, R., Zhang, Y., Li, Y., Xia, L., Guo, Y., Zhou, Q., 2020. Structural basis for the recognition of SARS-CoV-2 by full-length human ACE2. Sci. (80-.) 367, 1444–1448. https://doi.org/10.1126/science.abb2762.

Zhang, S., Liu, J., Jiang, D., Wuren, T., Ma, S., Du, Y., Yi, X., Wu, S., 2018. The plasma level changes of VEGF and soluble VEGF receptor-1 are associated with high-altitude pulmonary edema. J. Med. Invest 65, 64–68. https://doi.org/10.2152/jmi.65.64.

Zubieta-Calleja, G., 1989, High Altitude Pathology at 12000 Ft.

Zubieta-Calleja, G., Zubieta-DeUrioste, N., 2021a. The oxygen transport triad in high-altitude pulmonary edema: a perspective from the high andes. Int. J. Environ. Res. Public Health 18, 7619. https://doi.org/10.3390/ijerph18147619.

Zubieta-Calleja, G., Zubieta-DeUrioste, N., 2021b. Pneumolysis and "Silent Hypoxemia" in COVID-19. Indian J. Clin. Biochem. 36, 112–116. https://doi.org/10.1007/s12291-020-00935-0.

Zubieta-Calleja, G., Ardaya, G., Zubieta DeUrioste, N., Paulev, P., Zubieta-Castillo, G., 2013, Tolerance to hypoxia [WWW Document]. zuniv.net. URL ⟨https://zuniv.net/pub/ToleroncetoHypoxiaFiziol.pdf⟩.

Zubieta-Calleja, G., Zubieta-DeUrioste, N., Venkatesh, T., Das, K.K., Soliz, J., 2021. COVID-19 and Pneumolysis Simulating Extreme High-altitude Exposure with Altered Oxygen Transport Physiology; Multiple Diseases, and Scarce Need of Ventilators: Andean Condor's-eye-view. Rev. Recent Clin. Trials 15, 347–359. https://doi.org/10.2174/1574887115666200925141108.

Zubieta-Calleja, G.R., Zubieta-DeUrioste, N., 2022. High Altitude Pulmonary Edema, High Altitude Cerebral Edema, and Acute Mountain Sickness: an enhanced opinion from the High Andes – La Paz, Bolivia 3,500 m. Rev. Environ. Health. https://doi.org/10.1515/reveh-2021-0172.